AEM
Journals.ASM.org

Enhanced Biotransformation of Fluoranthene by Intertidally Derived *Cunninghamella elegans* under Biofilm-Based and Niche-Mimicking Conditions

Sayani Mitra,[a] Arnab Pramanik,[a] Srijoni Banerjee,[a] Saubhik Haldar,[b] Ratan Gachhui,[c] Joydeep Mukherjee[a]

School of Environmental Studies, Jadavpur University, Kolkata, India[a]; Department of Chemistry, Jadavpur University, Kolkata, India[b]; Department of Life Science and Biotechnology, Jadavpur University, Kolkata, India[c]

The aims of the investigation were to ascertain if surface attachment of *Cunninghamella elegans* and niche intertidal conditions provided in a bioreactor influenced biotransformation of fluoranthene by *C. elegans*. A newly designed polymethylmethacrylate (PMMA) conico-cylindrical flask (CCF) holding eight equidistantly spaced rectangular strips mounted radially on a circular disc allowed comparison of fluoranthene biotransformation between CCFs with a hydrophobic surface (PMMA-CCF) and a hydrophilic glass surface (GS-CCF) and a 500-ml Erlenmeyer flask (EF). Fluoranthene biotransformation was higher by 22-fold, biofilm growth was higher by 3-fold, and cytochrome P450 gene expression was higher by 2.1-fold when *C. elegans* was cultivated with 2% inoculum as biofilm culture in PMMA-CCF compared to planktonic culture in EF. Biotransformation was enhanced by 7-fold with 10% inoculum. The temporal pattern of biofilm progression based on three-channel fluorescence detection by confocal laser scanning microscopy demonstrated well-developed, stable biofilm with greater colocalization of fluoranthene within extracellular polymeric substances and filaments of the biofilm grown on PMMA in contrast to a glass surface. A bioreactor with discs rotating at 2 revolutions per day affording 6-hourly emersion and immersion mimicked the niche intertidal habitat of *C. elegans* and supported biofilm formation and transformation of fluoranthene. The amount of transformed metabolite was 3.5-fold, biofilm growth was 3-fold, and cytochrome P450 gene expression was 1.9-fold higher in the process mimicking the intertidal conditions than in a submerged process without disc rotation. In the CCF and reactor, where biofilm formation was comparatively greater, higher concentration of exopolysaccharides allowed increased mobilization of fluoranthene within the biofilm with consequential higher gene expression leading to enhanced volumetric productivity.

Polycyclic aromatic hydrocarbons (PAHs) are widespread in various ecosystems and are pollutants of great concern due to their potential toxicity, mutagenicity, and carcinogenicity. Microbial degradation represents the major mechanism responsible for the ecological recovery of PAH-contaminated sites. Fungi metabolize PAH compounds to metabolites similar to those formed by mammalian enzymes. The predominant pathway in the initial oxidation of PAHs is a cytochrome P450 (CYP) monooxygenase/epoxide hydrolase that catalyzes the reaction that forms *trans*-dihydrodiols. These metabolic steps are found in nonligninolytic fungi, such as *Cunninghamella elegans*, and the CYP genes are responsible for this biotransformation (1).

Fluoranthene (FA), a PAH containing four fused rings, occurs as a natural constituent of unaltered fossil fuels and is also formed during its combustion. The fungus *C. elegans* DSMZ 8217 metabolizes approximately 80% of the 3-^{14}C-labeled FA added within 72 h of incubation. The major pathway involves hydroxylation to form a glucoside conjugate of 3-hydroxyfluoranthene which accounts for 44.8% of the total transformed metabolites (2).

The primary routes of PAHs into estuarine environments include surface runoff, domestic or industrial effluents, petroleum spillage, and atmospheric deposition. PAHs accumulate to high concentrations in sediments and the tissues of estuarine organisms, especially in areas near their sources. Fluoranthene was identified as one of the principal PAHs found in the developed creek-salt marsh systems in the Charleston Harbor estuary as well as other developed estuaries (3, 4).

Intertidal microbial communities often occur as biofilms, which are high-density attached communities embedded in extracellular biopolymer matrices. In the fluctuating environments of intertidal systems, biofilms form protective microenvironments and may structure a range of microbial processes. Marine surface-associated microorganisms may require conditions that resemble their native environment in order to produce the maximum amount of bioactives; for example, studies have shown an increased production of antimicrobial compounds when the surface-associated bacteria were grown *in vitro* to form surface-attached biofilms (5, 6). In our previous studies, we showed that melanin production by estuarine bacterial isolate *Shewanella colwelliana*; endo-β-1,4-glucanase activity of another estuarine fungal isolate, *Chaetomium crispatum*; and riboflavin production by *Candida famata*, also an estuarine fungal isolate, were dependent upon biofilm formation (7–9).

The microorganism of the present study, *Cunninghamella elegans*, was obtained from estuarine mud of North Carolina. Although *C. elegans* is a ubiquitous fungus with a worldwide distribution pattern, it favors Mediterranean or subtropical climates and prefers to colonize the upper layers of moist soils. The biofilm phenotype is an increasingly important concept in mycological

Received 28 June 2013 Accepted 6 September 2013
Published ahead of print 13 September 2013
Address correspondence to Joydeep Mukherjee, joydeep_envstu@school.jdvu.ac.in.

doi:10.1128/AEM.02129-13

research. Very recently, the immobilization of *C. elegans* as a biofilm, for biotransformation of drugs to important human metabolites, was reported for the first time (10).

It may be hypothesized that surface attachment and biofilm formation of *C. elegans* can influence biotransformation of fluoranthene. Thus, it was our objective, first, to assess if surface attachment and biofilm formation by *C. elegans* enhance biotransformation of FA, which reportedly accumulates in the Charleston Harbor estuary (South Carolina). This fungus, coincidentally, was isolated from estuarine mud of North Carolina, approximately the same geographical location where FA accumulation has been reported. For this purpose, we applied our newly designed shaking flask, the conico-cylindrical flask (CCF) (S. Sarkar, D. Roy, and J. Mukherjee, U.S. patent application US2012/0295293A1) (see File S1 in the supplemental material at http://juenvmicrobiotech.org/AEMsuppl_matl.html), which provides substantially enhanced surface area as well as surface characteristics (hydrophobic/hydrophilic) for attachment of biofilm-forming microbes and at the same time provides a facility for varying the modes of aeration. A novel reactor system, the rotating disc bioreactor (RDBR), was used to mimic the niche environmental conditions of three salt-tolerant estuarine actinobacteria isolated from the Sundarbans region off the Bay of Bengal (11). The second objective was to verify if the niche intertidal conditions provided in this niche-mimicking bioreactor that rotates at an ultralow speed of 2 revolutions per day, providing 6-hourly emersion and immersion, affects the volumetric productivity (in terms of biotransformation capacity) of *C. elegans*.

MATERIALS AND METHODS

Microorganism. Stock cultures of the fungus *C. elegans* (DSM 8217, ATCC 36112) were maintained on potato dextrose agar plates and stored at 4°C.

Flask configurations and operating conditions. The conico-cylindrical flask (see Fig. S1 in the supplemental material at http://juenvmicrobiotech.org/AEMsuppl_matl.html) made of polymethylmethacrylate (PMMA-CCF), designed along with M/s Plastic Abhiyanta (India), is described elsewhere (7; Sarkar et al., U.S. patent application US2012/0295293A1). In the second configuration (GS-CCF), autoclaved glass slides were aseptically attached to both sides of the eight-strip inner arrangement. The surfaces of the inner arrangement of the CCFs were roughened, and roughness value (R_a) was determined with a profilometer. For sterilization, the CCF components were immersed in 2% (vol/vol) benzalkonium chloride for 5 h and then surface sterilized (7–9).

Ports on the top lid of the CCF were available for air inlet and exhaust. Three modes of aeration were examined in each of the three configurations: shaking at 140 rpm in an orbital shaker (with cotton plugs), orbital shaking with external aeration of 0.75 liter/min of air (through ports on top of the CCF), and external aeration under static condition. A standard unbaffled 500-ml Erlenmeyer flask (EF) made of borosilicate glass was the third flask configuration. Cultivation temperature of *C. elegans* was previously ascertained at 24°C (2).

Fluoranthene biotransformation in conico-cylindrical and Erlenmeyer flasks. Spores were washed from 3-day potato dextrose agar plates with 10 ml of 0.1% (vol/vol) Tween 80 solution, and 2 ml of homogenized cell suspension (approximately 10^7 spores per ml) was used as inoculum to aseptically inoculate different flasks (PMMA-CCF, GS-CCF, and EF) containing 100 ml Sabouraud dextrose broth (2). To prevent clumping of cells in the EF, the culturing method described previously (12) using 10% (vol/vol) inoculum was applied. The medium composition was as follows: enzymatic digest of casein, 5 g/liter; enzymatic digest of animal tissue, 5 g/liter; dextrose, 40 g/liter; distilled water, 1,000 ml; pH 5.6 ± 0.2. Fluoranthene (Sigma-Aldrich, USA; 0.2 mg dissolved in 20 μl of dimethyl sulfoxide) was added to each flask for induction of enzymes required for biotransformation. The different flask configurations were incubated with shaking at 140 rpm at 24°C. After 48 h of incubation, 80 mg of FA dissolved in 0.5 ml of dimethyl sulfoxide was added to each flask and the flasks were incubated for a further 72 h. As positive control, 80 mg of FA dissolved in 0.5 ml of dimethyl sulfoxide was incubated in 100 ml uninoculated Sabouraud dextrose broth for 120 h in all three flask configurations. As negative control, Sabouraud dextrose broth inoculated with *C. elegans* but without FA was used. Duplicate sets of three flask configurations were cultivated three times ($n = 6$).

Construction of the niche-mimicking rotating disc bioreactor (RDBR) and cultivation conditions. The 25-liter niche-mimicking reactor (see Fig. S2 in the supplemental material at http://juenvmicrobiotech.org/AEMsuppl_matl.html) made of polymethylmethacrylate was designed along with M/s Plastic Abhiyanta. A thin layer (2 to 3 mm) of hydrophobic polyurethane foam was attached to the disc surfaces to facilitate surface attachment of *C. elegans*. The reactor has a coaxial shaft on which a maximum of 10 discs can be mounted, and we used eight. The shaft was rotated at an ultralow speed of 2 rotations per day. At this rotational speed, when operated with half the tank filled with liquid medium, the discs would remain exposed to air and submerged in the medium alternatively for 6 h each, thus mimicking the niche semidiurnal tidal conditions of the location (North Carolina coast) from where *C. elegans* was collected. The reactor was disinfected by repeated washing with 2% (vol/vol) benzalkonium chloride and exposure to UV light by a lamp on the top of the reactor. Sterile air (0.20 to 0.24, vol/vol/min) was supplied to the RDBR by an air compressor and passage through a 0.22-μm air filter (Pall Corporation, USA). The supplied air was uniformly dispersed into the medium by a rectangular sparger having uniformly spaced holes. Ports on the top lid of the reactor were available for sampling, addition of medium, inoculum, pH measurement (PH-2 electrode, connected with pH controller FC-2000; Eyela, Japan), dissolved oxygen (DO) measurement (DO-2 electrode connected with DO controller FM-2000; Eyela, Japan), and temperature recording by a sensor connected to the pH controller as well as air exhaust. The process was run without pH control. Data were acquired with Eyela system software (ESS) and displayed online. Approximately 10^7 spores per ml medium were used as inoculum, and the RDBR was operated in the batch mode with a 12.5-liter working volume. The bioprocess medium composition was identical to the one used earlier in the CCF study. At the start of the cultivation, 25 mg of FA dissolved in 1 ml of dimethyl sulfoxide was added for induction of enzymes required for biotransformation. The biofilm was allowed to grow for 5 days, following which 10 g FA dissolved in 60 ml of dimethyl sulfoxide was added to the RDBR and run for a further 5 days. In the first process, the shaft was rotated at an ultralow speed of 2 rotations per day to mimic the semidiurnal tidal conditions. This was compared with another process where the semidiurnal niche-mimicking condition was not created by keeping the ultralow-speed rotating motor turned off throughout the cultivation period. Biofilm was allowed to form, and FA was added similarly as discussed above. In the RDBR experiments, two controls, one where FA was not added (a) and one where FA was added (b), were applied during cultivation of *C. elegans* under both operating conditions. Four cultivations in the two modes of bioreactor operation were carried out ($n = 4$).

Extent of biotransformation in biofilm, cell mass, and broth. The extent of FA biotransformation was estimated by measuring the amount of the major metabolite formed (3-fluoranthene-β-glucopyranoside [3-FG]). The biofilm scraped off the conico-cylindrical flasks and reactor discs as well as the cell mass recovered from Erlenmeyer flask cultures was separately extracted with 3 equal volumes of ethyl acetate (2). The spent culture broth (100 ml) of each flask as well as the reactor vessel (1,000 ml) was separately subjected to liquid-liquid extraction with 3 equal volumes of ethyl acetate. The control flask containing FA without the fungus and the other control flask with the fungus but without FA were extracted similarly with ethyl acetate. Analogous procedures were followed for the

control experiments carried out in the RDBR. The initial extracts were dried over anhydrous sodium sulfate, and the solvent was evaporated under reduced pressure at 38°C. The dried residues of the flasks were weighed and dissolved in methanol to prepare final extracts of equal concentrations (200 mg/ml) for thin-layer chromatography (TLC).

TLC analysis of extracts of biofilm, biomass, and extracellular broth. TLC was performed on silica gel plates (TLC aluminum sheets; Silica Gel 60 F_{254}; Merck, USA). The solvent system used was benzene-ethanol (9:1, vol/vol) (2). TLC chromatograms of the final extracts of the CCFs (of biofilm, biomass, and extracellular broth) were compared with the chromatograms of the extracts of the Erlenmeyer flask by observation at 254 and 365 nm. Similarly, final extracts of biofilm and extracellular broth obtained from the RDBR process run with shaft rotation were compared with the one without rotation. Preparative TLC was performed with the final extracts of all flask configurations and bioreactor operating conditions. The major transformed metabolite observed near the origin of the chromatograms was extracted from the silica gel with methanol for subsequent analyses.

NMR, mass spectroscopy (MS), and high-performance liquid chromatography (HPLC) analysis of the major biotransformed metabolite. The ^{1}H nuclear magnetic resonance (NMR) measurements were carried out on a Bruker Avance 600-MHz NMR spectrometer with a TCI cryoprobe at 25°C. The metabolite was dissolved in deuterated methanol (CD_3OD, 99.8 atom% D). Chemical shifts are reported in parts per million (ppm) by assigning the CH_3OD and CD_3OH resonances to 4.86 ppm and 3.31 ppm, respectively. The mass spectrometer (Jeol MStation, JMS-700) was operated in the electron impact (EI) ionization mode with a source temperature of 200°C and electron energy of 70 eV. The ionizing current applied was 100 μA, while the linear scan program was set at *m/z* 50 to 800.

The extracts of the CCFs, EF, and different bioreactor operating conditions obtained after preparative TLC were analyzed by reversed-phase HPLC in a high-pressure liquid chromatograph (Shimadzu, Japan) equipped with a photodiode array (PDA) detector (SPD-M20A) and fitted with a 100-Å LC column, 30 by 2.0 mm (Phenomenex, USA). The elution was programmed as follows: 20-min linear gradient of acetonitrile-water (10:90 to 100:0, vol/vol), followed by 100% acetonitrile for 5 min. The flow rate was maintained at 1.0 ml/min (13). For calculation of standard deviations (SDs), *n* was 6 for any flask configuration and *n* was 4 for any bioreactor operating condition.

Determination of cell surface hydrophobicity. Cell surface hydrophobicity was determined by the microbial adhesion to hydrocarbons (MATH) assay according to the work of Smith et al. (14) and as applied in reference 8. In this assay, cell suspensions with hydrophobic indexes greater than 0.7 were considered hydrophobic. All measurements described in this section were performed three times in duplicate sets ($n = 6$).

Measurement of biomass in the EF and biofilm in the CCFs and bioreactor. In this and the subsections below, measurements were made in the EF and CCFs inoculated with 2% (vol/vol) inoculum. Biomass was measured by vacuum filtering the mycelial mass formed in the EF, while biofilm formation was quantified by scraping off the total surface of the inner arrangement of the CCFs and discs of the bioreactor with a sharp scalpel at the end of the experiment. Cell masses of the EF and CCFs were dried to constant weight at 40°C and weighed. For calculation of standard deviation (SD), *n* was 6 for any flask configuration and *n* was 4 for any bioreactor operating condition.

Measurement of planktonic growth in the CCFs and bioreactor. At the end of the cultivation, spent medium (100 ml) of the CCFs as well as 1,000 ml of the RDBR was centrifuged at 10,000 rpm (Eppendorf 5810R, rotor F-34-6-38). The pellet was collected, dried at 40°C to constant weight, and weighed. For calculation of SD, *n* was 6 for any flask configuration and *n* was 4 for any bioreactor operating condition.

Measurement of EPS-polysaccharide concentration of biofilm and EF biomass. Polysaccharide contents of biomass of the EF and biofilm exopolymeric substances (EPS) of the CCFs and bioreactor (0.25 g) were determined according to the method in reference 15 and as adopted in reference 9. For calculation of SD, *n* was 6 for any flask configuration and *n* was 4 for any bioreactor operating condition.

CLSM. Biofilm architecture was determined by confocal laser scanning microscopy (CLSM) using slides as described previously (8, 9). Two sets of three flasks each were utilized during cultivation on PMMA as well as glass surfaces. Slides were aseptically taken out (two each) 1 day after addition of FA, i.e., the 4th, 5th, and 6th days of cultivation, and washed twice with phosphate-buffered saline (PBS) buffer (8, 9). EPS staining with fluorescein isothiocyanate-concanavalin A (FITC-ConA; Sigma, USA) was done as explained elsewhere (8, 9). Thereafter, slides were incubated with SYTO 64 (Molecular Probes, USA) as elucidated previously (8, 9). Biofilm development was visualized in an Olympus IX81 (Japan) confocal laser scanning microscope with Fluoview FV1000 software equipped with argon and helium-neon lasers. A plan-APO 40 by 1.35 numerical aperture (NA) oil-immersion lens was used as the objective. Image stacks were collected under identical conditions (i.e., similar area and vertical resolution) at 1-μm z-intervals. For visualization of FA, excitation was fixed at 405 nm and emission at 460 nm; for observation of FITC-ConA, excitation was set at 488 nm and emission at 520 nm; and for visualization of SYTO 64, excitation was fixed at 543 nm and emission at 620 nm. Experiments were performed three times in duplicate sets ($n = 12$).

Image analysis. PHLIP software (16) was applied for three-dimensional (3D) biofilm analysis as described previously (8, 9). In this work, PHLIP calculations with three-channel CLSM data (FITC-ConA, SYTO 64, and fluoranthene) were used to determine the total biovolume, mean thickness, substratum coverage, total spreading, roughness coefficient, surface area-to-biovolume ratio, fractal dimension in two dimensions (2D), and colocalization in 3D according to references 8 and 9. Data were exported in an HTML format and were statistically analyzed using Origin. ImageJ was used for processing the image stacks using the Volume Viewer 1.31. Three-dimensional surface plots of the biofilm were constructed using the interactive 3D surface plot plug-in 2.32 of ImageJ (8, 9, 16, 17).

Preparation of total RNA of biofilm and biomass cells. The biofilm scraped off the CCFs and reactor discs and the cell mass recovered from EF cultures (200 mg) were separately ground in liquid nitrogen. Total RNA was extracted using the TRIzol reagent (Invitrogen, USA) according to the manufacturer's instructions. RNA pellets were dissolved in diethyl pyrocarbonate-treated water, and their concentrations and purity were determined spectrophotometrically (Lambda 25; Perkin-Elmer, USA). The 260/280 ratios were greater than 1.8.

Expression analysis of CYP gene. From 2.5 μg of total RNA isolated from CCFs, the EF, and different bioreactor operating conditions, cDNA was synthesized by random hexamers (50 ng/μl) using the Superscript first-strand synthesis kit for reverse transcriptase PCR (RT-PCR) (Invitrogen, USA) according to the manufacturer's protocol. Two microliters from each RT reaction mixture was amplified in a 25-μl PCR mix using the primers 5′-GGT ATG AAC TTT AGT TTA TTA GAA CAA-3′ and 5′-CGG ATT TTC AAA TCA ATT GGT TTA GGT-3′ specific for CYP (18). To ensure that there was no DNA contamination and to normalize RT-PCR results, PCR and RT-PCR against each RNA sample were performed parallel with universal primers LR0R and LR5 targeting 28S rRNA of fungi (19). Gel images were taken by UVIpro Platinum gel documentation systems (UVItec, United Kingdom). Bands of about 148-bp amplicons in a 35-cycle PCR for CYP and about 900-bp amplicons in a 35-cycle PCR for 28S rRNA were analyzed by the ImageJ program.

RESULTS

Identity of the major transformed metabolite. The TLC chromatograms of the final extracts of flasks (PMMA-CCF, GS-CCF, and EF) as well as those obtained from the RDBR experiments were compared at 254 and 365 nm. The major spots were identical as observed in the two wavelengths. Spots of the transformed metabolite from different flasks and bioreactor operating conditions

TABLE 1 Values of colocalization in 3D obtained through confocal laser scanning microscopy and image analysis during biofilm cultivation of *C. elegans* on hydrophobic (PMMA) and hydrophilic (glass) surfaces[a]

	Day 4		Day 5		Day 6	
Channel pair	PMMA-CCF	GS-CCF	PMMA-CCF	GS-CCF	PMMA-CCF	GS-CCF
Blue-green	39.77 ± 5.94	40.55 ± 6.87	67.69 ± 9.37	27.83 ± 4.47	50.71 ± 8.48	39.63 ± 5.82
Blue-red	14.4 ± 2.68	3.92 ± 0.78	59.33 ± 10.56	44.36 ± 7.27	54.88 ± 8.58	22.19 ± 3.45

[a] Blue channel, fluoranthene; green channel, exopolymeric substances (EPS); red channel, whole cells. Error ranges indicate 1 standard deviation from the mean.

were identified near the origin ($R_f = 0.12$), as no such spot was present in the controls.

The ^{1}H NMR spectrum of the transformed metabolite consisted of characteristic aliphatic resonance, from δ 3.47 to 3.96, corresponding to a glucose unit as well as an aromatic region, from δ 7.31 to 8.24, corresponding to the FA ring. In the aliphatic region, the most up-field signal, δ 3.47 to 3.49 (m, 1H), corresponded to the 4′ proton of the glucose unit. Another signal at δ 3.53 to 3.56 (m, 2H) corresponded to 5′ and 3′ protons. However, the 2′ proton showed a proton multiplet at δ 3.657 to 3.67. The diastereomeric 6′ protons showed two multiplets, one at δ 3.75 to 3.78 (m, 1H) and another at δ 3.93 to 3.96 (m, 1H). The presence of a β-glucopyranose ring was confirmed by the proton doublet at δ 5.17 ($J = 7.8$ Hz) which was analogous to previously reported data of δ 5.18 (d, 1H, $J = 7.7$ Hz) (2). The signals for Hs of C-2, C-8, and C-9 of the FA ring were found at δ 7.31 to 7.35 (m, 3H). The proton at C-5 showed a signal at δ 7.62 to 7.65 (m, 1H). However, signals for C-10, C-1, and C-7 were found as three closely spaced doublets at δ 7.87 (d, 1H, $J = 7.2$ Hz), δ 7.91 (d, 1H, $J = 7.8$ Hz), and δ 7.92 (d, 1H, $J = 7.2$ Hz), respectively. The C-6 and C-4 protons of the FA ring showed signals at δ 8.00 (d, 1H, $J = 8.4$ Hz) and at δ 8.24 (d, 1H, $J = 6.6$ Hz). Apparently, the coupling pattern in the aromatic region suggested that the substitution took place at the C-3 position as the symmetrical resonance signal of the unsubstituted FA ring was not obtained in the metabolite. Integration corresponded to ^{1}H at the C-4 atom and showed equal value to the β-hydrogen atom at the C-1′ of the glucose unit, suggesting a monofunctionalization of the glucose unit on the FA ring. The MS analysis also confirmed the above result showing *m/z* 218 [M^+ − Glu] and *m/z* 189 [M^+ − Glu − HCO] as obtained previously (2). Thus, the identity of the transformed metabolite was 3-fluoranthene-β-glucopyranoside, as reported earlier (2).

Effect of aeration, flask configuration, and surface property on fluoranthene biotransformation and biofilm formation by *C. elegans*. The roughness average R_a (PMMA) was estimated as 2.51 ± 0.05 μm (1 standard deviation, $n = 15$), while R_a (glass) was determined to be 2.43 ± 0.02 μm (1 standard deviation, $n = 15$). Thus, the two materials were of almost equal roughness.

Orbital shaking at 140 rpm was found to be optimal for fluoranthene biotransformation by *C. elegans* in EF, PMMA-CCF, and GS-CCF. Shaking with external aeration as well as external aeration under the static condition did not enhance the biotransformation of FA (see Table S1 in the supplemental material at http://juenvmicrobiotech.org/AEMsuppl_matl.html).

In cultivations with shaking at 140 rpm, the highest transformation of FA to 3-FG by biofilm cells (3-FG = 1.113 ± 0.061 mM) as well as biofilm formation (1.36 ± 0.07 g [dry weight] biofilm) and biofilm EPS polysaccharide content (364.7 ± 19.0 μg/ml) occurred in the hydrophobic PMMA surface vessel (PMMA-CCF) followed by the hydrophilic surface vessel (GS-CCF) (3-FG = 0.241 ± 0.022 mM; 0.965 ± 0.06 g [dry weight] biofilm; 203.7 ± 11.0 μg/ml biofilm EPS polysaccharide content) and finally the EF (3-FG = 0.051 ± 0.003 mM; 0.46 ± 0.03 g [dry weight] cell; 85.8 ± 5.0 μg/ml EPS polysaccharide content). In the extracellular broth of PMMA-CCF, the concentration of 3-FG was the highest (2.797 ± 0.113 mM) compared to the GS-CCF (0.554 ± 0.030 mM) and the EF (0.520 ± 0.020 mM). Thus, a 22-fold increase (considering biofilm cells) and a 5-fold increase (considering extracellular broth) in biotransformation were obtained when *C. elegans* grew as biofilm culture in the PMMA-CCF in comparison to the traditional cultivation in the EF. Planktonic growth was negligible (0.0002 ± 0.00005 g dry cell biomass in the PMMA-CCF and 0.0001 ± 0.00005 g dry cell biomass in the GS-CCF) in the cultivations performed in the CCF that allowed biofilm formation. In cultivations with a 10% inoculum, biotransformation in the EF was 46% higher in contrast to that observed with a 2% inoculum (3-FG = 0.111 ± 0.006 mM in biomass). However, even with a larger amount of inoculum, biotransformations in the CCFs were higher than the biotransformation in the EF. The concentration of 3-FG in biofilm cells of the PMMA-CCF was 0.765 ± 0.062 mM while that of the GS-CCF was 0.121 ± 0.007 mM. Thus, biotransformation in the PMMA-CCF was higher than that in the EF by 7-fold with a 10% (vol/vol) inoculum. The cell surface hydrophobicity of *C. elegans* was estimated as 0.83 ± 0.01, indicating the cell surfaces to be hydrophobic and possessing higher affinity for the PMMA surface than the glass surface. Error ranges indicate 1 standard deviation from the mean. These results not only point toward a strong correlation between the hydrophobic reactor surface, biofilm formation, and biotransformation by *C. elegans* but also suggest that biofilm cultures were more productive (in terms of extent of biotransformation) than cultivation in traditional EF.

Confocal laser scanning microscopy of *C. elegans* biofilm. Data on biofilm architecture of the 4th to the 6th days are presented elsewhere (see Fig. S3 in the supplemental material at http://juenvmicrobiotech.org/AEMsuppl_matl.html). Biovolume, mean thickness, and substratum coverage values of the biofilm on the PMMA surface were higher than that of the film on the glass surface at comparable times (data not shown). Values of total spreading were comparable on the two surfaces. Data for surface area/biovolume ratio implied that the PMMA biofilm adapted more stably than the glass biofilm. The decrease of the roughness coefficient of the PMMA biofilm indicated that the film assumed an ordered structure while the glass biofilm remained more or less nonheterogenous. 2D fractal dimension values (which indicate the irregularity of the object perimeter) were comparable for the two surfaces.

The colocalization in the 3D operation calculates the percentage of overlapping biovolume in two selected channels (16). Table 1 shows the values of colocalization in 3D for *C. elegans* biofilm grown on hydrophobic (PMMA) and hydrophilic (glass) surfaces. Generally, colocalization values of blue channel-green channel as

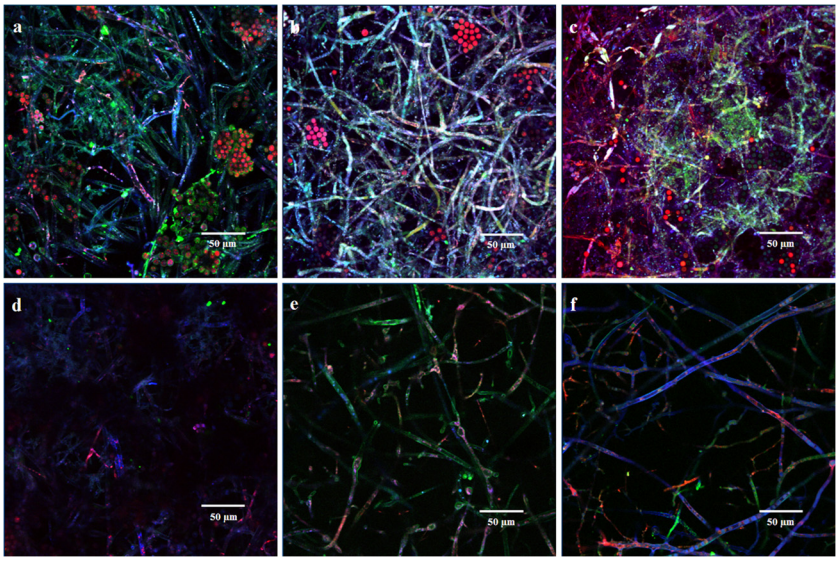

FIG 1 Typical CLSM micrograph of *C. elegans* biofilm following analysis by ImageJ using the Volume Viewer 1.31 plug-in and observed in the *x-y* plane after 4 (a), 5 (b), and 6 (c) days on PMMA surface and 4 (d), 5 (e), and 6 (f) days on glass surface.

well as blue channel-red channel were always higher in biofilms grown on the PMMA surface than in the film developed on the glass surface. This identified a preferential spatial association of FA with *C. elegans* grown on the hydrophobic surface in relation to the association of fluoranthene with the fungus grown on the hydrophilic surface. On day 4, more FA was associated externally with the EPS than within the cells as shown by the blue channel-green channel colocalization values. As time progressed, blue channel-red channel colocalization values increased, indicating transition of association from external EPS to the intracellular regions of the cell.

As evident from Fig. 1a to c, the appearance of strong blue, green, and red fluorescence indicated development of a stable biofilm on PMMA along with colocalization of FA in the EPS and filaments in contrast to the reduced biofilm formation on glass (Fig. 1d to f). Considering the similarity to biofilm growth of other zygomycetes fungi, it may be said that the intertwining of the mycelial mass provided stability and integrity to the biofilms and was achieved by extensive branching, followed by elongation of the hyphal branches by apical growth (20). Three-dimensional surface plots of the biofilm growing on the PMMA surface (see Fig. S4a to c in the supplemental material at http://juenvmicrobiotech.org/AEMsuppl_matl.html) showed colocalization of FA as well as increasing fluorescence intensity of the fluorophores along with progression of time. Patchy biofilms developed when *C. elegans* grew on the glass surface in contrast to the PMMA surface biofilm, whose projected 3D biofilm surface was spread more widely along the section (Fig. S4d to f). Thus, the ImageJ analysis in conjunction with the biofilm architectural parameters demonstrated robust development of *C. elegans* biofilm on the PMMA surface but not on the glass surface.

Cultivation in the RDBR. In cultivations with rotation that mimicked the niche intertidal conditions where *C. elegans* was immersed in water for 6 h and exposed to air for 6 h, the biofilm developed uniformly and spread out as a mat over the discs (see Fig. S2b and c in the supplemental material at http://juenvmicrobiotech.org/AEMsuppl_matl.html). In contrast, the amount of attached growth was smaller when the shaft was not rotated and *C. elegans* was totally submerged in water and not exposed to air intermittently for 6 h (Fig. S2d). Figure 2 shows that the minimum partial O_2 pressure (pO_2) level was 60% saturation when *C. elegans* was cultivated with shaft rotation while the minimum pO_2 level was 40% saturation when the fungus was cultivated without shaft rotation. In the latter process, the pO_2 level dropped below 20% saturation at 180 h and aeration was stepped up by 0.5 liter/min. The medium pH decreased from 5.6 to 5.4 in the niche-mimicking process whereas the medium pH declined more rapidly from 5.7 to 5.0 in the process not simulating the intertidal environment. The medium temperature remained between 24 and 26°C for both modes of cultivation.

When the discs were rotated, the amount of biofilm formed was 12.47 ± 0.7 g, which was much larger than the amount of

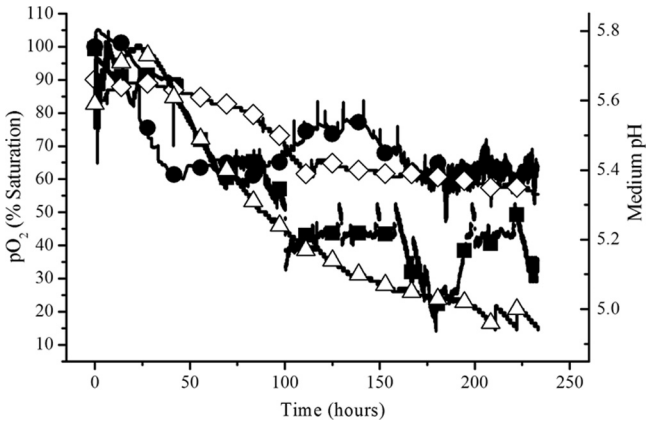

FIG 2 Dissolved oxygen and medium pH profiles during fluoranthene biotransformation by *C. elegans* in the rotating disc bioreactor. Filled circles, pO_2 in process mimicking the intertidal conditions; filled squares, pO_2 in submerged process without disc rotation; open diamonds, pH in process mimicking the intertidal conditions; open triangles, pH in submerged process without disc rotation.

TABLE 2 Growth parameters of *C. elegans* during biotransformation of fluoranthene in the RDBR[a]

RDBR process condition	Biomass (g)	Growth rate (g/h)	Volumetric productivity (mM/liter)		Specific productivity (mM/g of biomass)	
			Biofilm cells	Extracellular broth	Biofilm cells	Extracellular broth
Niche mimicking (with shaft rotation)	12.47 ± 0.70	0.050 ± 0.005	0.072 ± 0.004	0.169 ± 0.014	0.072 ± 0.001	0.169 ± 0.005
Submerged (without shaft rotation)	4.0 ± 0.3	0.014 ± 0.001	0.021 ± 0.003	0.038 ± 0.006	0.065 ± 0.005	0.118 ± 0.010

[a] Productivities were calculated based on 3-fluoranthene-β-glucopyranoside concentrations (mM), the volume of medium was 12.5 liters, and the growth period was 230 h. Error ranges indicate 1 standard deviation from the mean.

biofilm formed (4.0 ± 0.3 g) when the discs were stationary. Planktonic growth was 0.025 ± 0.001 g (in 12.5 liters of medium) in the process with disc rotation while 0.037 ± 0.001 g was recorded for the process without shaft rotation. Thus, planktonic growth was very modest compared to biofilm growth. Similarly, the polysaccharide content of the EPS obtained from the biofilm formed when *C. elegans* was cultivated under the intertidal niche-mimicking condition (346.3 ± 17.9 μg/ml) was higher than that obtained when *C. elegans* was not cultivated under the condition allowing periodic immersion and emersion (183.3 ± 9.4 μg/ml). The amount of 3-FG obtained under the intertidal niche-mimicking condition was larger by 3.5 to 4.5 times than that recovered under the condition not allowing periodic wetting and drying. In the process run with shaft rotation, the concentration of 3-FG was 0.902 ± 0.046 mM, compared to 0.259 ± 0.037 mM obtained in the process run without shaft rotation. In the extracellular broth, likewise, the concentration of 3-FG obtained in the process with shaft rotation (2.111 ± 0.178 mM) was much higher, in contrast to 0.475 ± 0.072 mM recovered from the process without shaft rotation. Error ranges indicate 1 standard deviation from the mean. Table 2 shows that biomass was greater by 3-fold under the niche-mimicking condition than under the submerged condition. Consequentially, the growth rate was higher by 3.5-fold. The process with shaft rotation showed enhanced volumetric productivities compared to the one without rotation by 3.4- to 4.5-fold. Specific productivities increased by 1.1- to 1.4-fold.

Expression analysis of CYP gene. Based on the highly conserved heme-binding regions (21, 22), the differential expression of the CYP gene in *C. elegans* biomass of the EF and biofilm of the PMMA-CCF and GS-CCF as well as different bioreactor operating conditions was determined by semiquantitative RT-PCR. Products of the expected size (approximately 148 bp) from the PCR were detected on an agarose gel after RT-PCR with total RNA extracted from the biomass of the EF and biofilms of the CCFs as well as reactor discs indicating the presence of cytochrome P450 mRNA. The RT-PCR results (Fig. 3) show that the CYP mRNA level was enhanced by 2.1-fold in the biofilm of *C. elegans* cultivated in the PMMA-CCF compared to that in the cell mass of EF. The mRNA level in the biofilm of GS-CCF was equal to the level obtained in the cell mass of EF (Fig. 3). From the results, it is clear that biofilm cultivation on a hydrophobic PMMA surface enhanced the expression of the cytochrome P450 gene. However, biofilm grown on a hydrophilic glass surface did not provide any increment to gene expression compared to that obtained in the EF. Thus, a hydrophobic surface for cell attachment resulted in differential gene expression in *C. elegans* biofilm. In the bioprocesses operated in this study, the CYP mRNA level was increased by 1.9-fold in the biofilm extracted from the RDBR cultivated under the niche-mimicking condition compared to the biofilm obtained from the RDBR operated under the submerged condition (Fig. 3). The expression of the 28S rRNA gene (the housekeeping gene) remained constant in all flasks and under all bioreactor operating conditions.

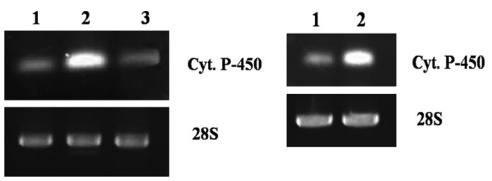

FIG 3 Expression analysis of cytochrome P450 (upper panel) and 28S rRNA (lower panel) during cultivation of *C. elegans* with fluoranthene in various flasks (left), EF (lane 1), PMMA-CCF (lane 2), and GS-CCF (lane 3), and RDBR (right), without shaft rotation (lane 1) and with shaft rotation (lane 2), as determined by semiquantitative RT-PCR.

DISCUSSION

In this study, the effect of flask configuration on fluoranthene biotransformation by *C. elegans* as well as the effect of niche environmental conditions during bioreactor cultivation on volumetric productivity (in terms of extent of biotransformation) was researched.

The fungus, having an inherently hydrophobic cell surface character, had more affinity for the hydrophobic reactor surface. This led to higher numbers of cells attaching to the PMMA and consequentially higher biofilm formation on this surface in comparison to the glass surface, which has a hydrophilic characteristic. Colocalization values indicated more availability of FA to the cells grown on the hydrophobic surface in contrast to those grown on the hydrophilic surface. Owing to increased amounts of FA available for biotransformation, CYP gene expression was higher in the PMMA-CCF than in the GS-CCF. The greater extent of biotransformation observed in the GS-CCF than in the EF was due to the higher biomass and increased bioavailability of fluoranthene mediated through biofilm formation. From previous knowledge (23), it can be assumed that membrane-bound cytochrome P450 enzymes were responsible for this biotransformation. Thus, a positive relationship between cell surface hydrophobicity, reactor vessel surface hydrophobic characteristic, biofilm formation, biotransformation, and resultant CYP gene expression was established in *C. elegans*.

The fungus grew as scattered clumps in the EF when cultured with a small inoculum. Greater inoculum size inhibited clumping and increased biotransformation in the EF, but the extent of biotransformation remained greater in the CCFs than in the EF as observed with a smaller inoculum size. Fungal morphological

variations occurred when *C. elegans* was grown in the presence of solid supports (24). In general, the fungal mycelium tended to aggregate as one big pellet. This morphological form appeared to be common when grown without any solid support. Use of solid supports such as activated carbon and Florisil enhanced the biotransformation efficiency. In our experiments, growth was mostly planktonic in the EF while negligible planktonic growth was observed in the CCF. Although the external medium remained clear during the experiments, indicating very little cell detachment, it was also likely that some detachment also occurred during the experiment and the detached cells may be partially responsible for fluoranthene biotransformation observed as noted elsewhere (10). The fundamental method prescribed previously (2) was followed in this study, where the mycelia were extracted to recover the biotransformed metabolites but not the spent medium. We, nevertheless, analyzed the spent medium and found the concentration of the transformed metabolite to be higher than or nearly equal to that in the extracellular milieu compared to biofilm cells. Planktonic growth was 0.015 to 0.01% of biofilm growth. The very small amount of planktonic cell mass cannot generate a significant amount of 3-FG in the extracellular milieu, given that FA was added after biofilm formation. So, we believe that after biotransformation within the biofilm cells, the transformed metabolite was released in the extracellular broth. Therefore, this communication is focused on fluoranthene biotransformation within the biofilm. This approach is supported by the results (10) where cells embedded in biofilm played the predominant role in drug metabolism in microtiter plates. The authors also found it interesting that fungal cells immobilized as biofilm were able to convert flurbiprofen more efficiently than were nonattached filamentous hyphae, suggesting increased CYP activity in biofilm (10). However, CYP gene expression was not demonstrated by the authors as reported in this communication. Surface type impacted biofilm formation of *C. elegans* as observed previously (10), although the authors did not investigate the effect of vessel surface hydrophilicity/hydrophobicity as described in this article. The natural tendency of filamentous fungi is to grow adherent to surfaces, and the submerged free-floating growth is not a fungal natural way of living (25). The novel design of the CCF with enhanced surface area permitted natural growth, producing higher biomass in comparison to the EF, and thus, the CCF was a better reaction vessel in terms of volumetric productivity. Specific productivity (in terms of unit biomass) was not considered, as the observed enhancement was more of a "biofilm-biomass" effect than increased efficiency of the cells forming the biofilm.

Hydrophobic bacteria may be easily expelled from the water phase due to unfavorable energetic effects and seek contact with the hydrophobic surfaces (26). The rate of substrate flux to a bacterial cell is determined by the substrate concentration gradient, which becomes steeper as a cell approaches a surface with sorbed substrate, and this increased substrate concentration permits greater activity of attached cells than suspended cells including the functioning of extracellular hydrolytic enzymes (27–29). When the solid phase provides poor sorption properties, the evolution of a microbial biofilm on its surface may provide an important sink and reservoir for hydrophobic contaminants delivered by the aqueous phase (30). Biofilms can form a significant sink for hydrophobic organic contaminants (HOCs) in systems with low organic carbon content and high surface areas (31). It can be assumed that PMMA and glass surfaces, neither of which have good sorption properties, together with the enhanced surface area of the CCF provided the opportune conditions for biofilm formation. The biofilm so formed by *C. elegans* acted as a sink (reservoir) for fluoranthene. To the best of our knowledge, no literature exists on the comprehensive explanation for enhanced bioactivity observed in attached fungal cells in biofilms in contrast to planktonic cultures. In its absence, the body of literature on bacterial biofilm presented here may be considered the most likely explanations, given that the models of biofilm development in bacteria, yeasts, and filamentous fungi are essentially similar (32).

Fungi can be considered regular biofilm-forming organisms with two inherent and fundamental processes: adhesion and subsequent differential gene expression (33). Transcription of both exoglucanase (*exo*) and xylanase (*xynB*) genes were higher in the biofilm culture than in the submerged culture of *Aspergillus niger* ATCC 10864 (34). Overexpression of the major CYP gene in the PMMA-CCF biofilm culture by 2.1-fold compared to the traditional EF culture in our study can be considered analogous to the enhanced expression of the principal *exo* and *xynB* genes of *A. niger* in biofilm culture. Harding et al. (32) discussed compelling evidence in support of the hypothesis that filamentous fungi are capable of forming biofilms, and a set of criteria for characterizing filamentous fungal biofilms was proposed. Through this investigation, successful satisfaction of those three criteria (32) was demonstrated: first, surface-associated growth of cells; second, cells embedded in a self-produced and secreted extracellular polymeric matrix; and third, altered gene expression.

Semiquantitative RT-PCR provides a highly sensitive and specific method to analyze gene expression, and this method was applied to *C. elegans* research to examine CYP gene (18) and CeCyt gene (19) expression. The technique, however, does not allow exact quantification of differences in expression levels of genes. The more accurate real-time quantitative RT-PCR, on the other hand, provides an exact determination of the number of mRNA molecules but is complex and costly (35). To date, no published methodology on real-time RT-PCR of *C. elegans* is available, so we relied on the already-established semiquantitative RT-PCR method. Analysis of CYP gene expression in *C. elegans* biomass and biofilm by real-time RT-PCR for exact quantification of transcripts is recommended.

The amount of biofilm formed and the extent of PAH biotransformed as well as the level of CYP gene expression were considerably greater in RDBR cultivations mimicking the niche intertidal conditions, where the fungus was cyclically exposed to air twice for 6 h and immersed in water twice for 6 h in a 24-h daily cycle. Considering the recent classification of fermentation systems, solid-state fermentation (SSF) is a process which involves the attached growth of microorganisms (mainly fungi) on moist solid substrates in the absence of free-flowing water. The main difference with biofilms is the quantity of liquid in the system being abundant in biofilms. Fermentation by filamentous fungal biofilms (FFB) is a homogeneous production system within a liquid environment based on the infrastructure of the SSF process with the productive efficiency of the SSF (25). So, the use of hydrophobic polyurethane foam in our experiments should not be considered cell immobilization or solid-state cultivation.

The niche-mimicking condition allowed 12-hourly aerial exposure per day, during which the water content was quite low and the microorganism was almost in contact with gaseous oxygen in the air, unlike in the case where the niche environmental condi-

tion was not mimicked. The water content was just sufficient to moisten the substrate, and no signs of biofilm desiccation (dryness and dehydration) were observed visually. The demand for DO was lower in the niche-mimicking process (in comparison to the process not mimicking the intertidal condition) as the fungus consumed oxygen from air during periodic aerial exposure (Fig. 2). Oxygen is more likely to limit the growth within the film than lack of glucose even when the outer edge of the biofilm is high in oxygen concentration (36). The fungal hyphae exposed directly to the air could probably take up oxygen directly from the air. The microorganism took oxygen directly in the places of the substrate where the water film was not present with consequential lower mass transfer resistance (37). O_2 was consumed, and CO_2, H_2O, heat, and biochemical products were produced. Hence, gradients developed within the biofilm that, for instance, forced O_2 to diffuse from the gaseous phase into deeper regions of the biofilm and CO_2 to diffuse from these regions to the gaseous phase (38). Thus, better mass transfer characteristics for oxygen obtained during periodic aerial exposures of *C. elegans* under the niche-mimicking condition allowed higher biofilm biomass formation. Greater enhancement of volumetric than specific productivities (Table 2) implied that the improved biotransformation under the niche-mimicking condition was a "biofilm-biomass" effect similar to that observed in the CCF. It was reported that in static well plates and flasks, *C. elegans* formed a mat with aerial hyphae at the liquid-air interface, strongly suggesting that oxygen availability played an important role in the formation of biofilm (10). Our experiments further ascertained increased CYP gene expression in *C. elegans* under the niche-mimicking condition. We presume that this enhancement was due to the increased availability of FA in the biofilm. The larger amount of exopolysaccharide in the biofilm grown under the niche-mimicking condition than under the condition not allowing periodic aerial exposure permitted greater amounts of FA to be mobilized into the biofilm for transformation, similar to the effect observed in the CCF study, hence the increased CYP gene expression. Thus, better mass transfer characteristics coupled with higher CYP gene expression contributed to the higher volumetric productivity (in this case biotransformation) of *C. elegans* under the niche-mimicking condition.

Conclusions. Through the application of the newly designed conico-cylindrical flask, it was shown that diverse extents of fluoranthene biotransformation and variable extents of cell adhesion and biofilm formation occurred when *C. elegans* was cultivated in differently constructed shaking vessels. These observations were attributed to the magnitude of differential CYP gene expression. The influence of vessel surface character on volumetric productivity of biofilm-forming *C. elegans* has been highlighted for the first time. Previously, we demonstrated that the RDBR, operated at a rotational speed of 1 revolution per day and 50% submergence of discs, faithfully mimicked the intertidal estuarine habitat of three marine isolates of the Sundarbans estuary (India) and supported biofilm formation and production of antimicrobial metabolites (11). This investigation and application of the niche-mimicking RDBR are now being extended to another geographical location (United States) where provision of niche intertidal conditions enhanced the extent of biotransformation and sustained biofilm formation. The observation was ascribed to enhanced mass transfer and increased CYP gene expression. Integrating the two objectives (as mentioned in the introduction) of this investigation, it can thus be concluded that biofilm formation on a hydrophobic surface with intermittent emersion and immersion in the fluid medium is the most suitable condition for biotransformation of FA by *C. elegans*. It would be interesting to see if the results obtained in this simulated study can be replicated in natural intertidal settings.

ACKNOWLEDGMENTS

Financial support of J.M. and R.G. (DBT sanction no. BT/PR11479/AAQ/03/423/2008) and S.M. [CSIR sanction no. 09/96(0764)/2013/EMR-I] is thankfully acknowledged.

We thank the CU-DBT-IPLS facility for confocal microscopy.

REFERENCES

1. **Peng RH, Xiong AS, Xue Y, Fu XY, Gao F, Zhao W, Tian YS, Yao QH.** 2008. Microbial biodegradation of polyaromatic hydrocarbons. FEMS Microbiol. Rev. **32:**927–955.
2. **Pothuluri JV, Freeman JP, Evans FE, Cerniglia CE.** 1990. Fungal transformation of fluoranthene. Appl. Environ. Microbiol. **56:**2974–2983.
3. **Weinstein JE, Sanger DM, Holland AF.** 2003. Bioaccumulation and toxicity of fluoranthene in the estuarine oligochaete *Monopylephorus rubroniveus*. Ecotoxicol. Environ. Saf. **55:**278–286.
4. **Weinstein JE, Sanger DM.** 2003. Comparative tolerance of two estuarine annelids to fluoranthene under normoxic and moderately hypoxic conditions. Mar. Environ. Res. **56:**637–648.
5. **Yan L, Boyd KG, Adams DR, Burgess JG.** 2003. Biofilm-specific cross-species induction of antimicrobial compounds in bacilli. Appl. Environ. Microbiol. **69:**3719–3727.
6. **Yan L, Boyd KG, Burgess JG.** 2002. Surface attachment induced production of antimicrobial compounds by marine epiphytic bacteria using modified roller bottle cultivation. Mar. Biotechnol. **4:**356–366.
7. **Mitra S, Sarkar S, Gachhui R, Mukherjee J.** 2011. A novel conico-cylindrical flask aids easy identification of critical process parameters for cultivation of marine bacteria. Appl. Microbiol. Biotechnol. **90:**321–330.
8. **Mitra S, Banerjee P, Gachhui R, Mukherjee J.** 2011. Cellulase and xylanase activity in relation to biofilm formation by two intertidal filamentous fungi in a novel polymethylmethacrylate conico-cylindrical flask. Bioprocess Biosyst. Eng. **34:**1087–1101.
9. **Mitra S, Thawrani D, Banerjee P, Gachhui R, Mukherjee J.** 2012. Induced biofilm cultivation enhances riboflavin production by an intertidally derived *Candida famata*. Appl. Biochem. Biotechnol. **166:**1991–2006.
10. **Amadio J, Casey E, Murphy CD.** 2013. Filamentous fungal biofilm for production of human drug metabolites. Appl. Microbiol. Biotechnol. **97:**5955–5963.
11. **Sarkar S, Saha M, Roy D, Jaisankar P, Das S, Roy LG, Gachhui R, Sen T, Mukherjee J.** 2008. Enhanced production of antimicrobial compounds by three salt-tolerant actinobacterial strains isolated from the Sundarbans in a niche-mimic bioreactor. Mar. Biotechnol. **10:**518–526.
12. **Amadio J, Murphy CD.** 2010. Biotransformation of fluorobiphenyl by *Cunninghamella elegans*. Appl. Microbiol. Biotechnol. **86:**345–351.
13. **Lambert M, Kremer S, Sterner O, Anke H.** 1994. Metabolism of pyrene by the basidiomycete *Crinipellis stipitaria* and identification of pyrenequinones and their hydroxylated precursors in strain JK375. Appl. Environ. Microbiol. **60:**3597–3601.
14. **Smith SN, Chohan R, Armstrong RA, Whipps JM.** 1998. Hydrophobicity and surface electrostatic charge of conidia of the mycoparasite *Coniothyrium minitans*. Mycol. Res. **102:**243–249.
15. **Paramonova E, Krom BP, van der Mei HC, Busscher HJ, Sharma PK.** 2009. Hyphal content determines the compression strength of *Candida albicans* biofilms. Microbiology **155:**1997–2003.
16. **Mueller LN, De Brouwer JFC, Almeida JS, Stal LJ, Xavier JB.** 2006. Analysis of a marine phototrophic biofilm by confocal laser scanning microscopy using the new image quantification software PHLIP. BMC Ecol. **6:**1–15.
17. **Eshed L, Yaron S, Dosoretz CG.** 2008. Effect of permeate drag force on the development of a biofouling layer in a pressure-driven membrane separation system. Appl. Environ. Microbiol. **74:**7338–7347.
18. **Lisowska K, Szemraj J, Rózalska S, Długoński J.** 2006. The expression of cytochrome P-450 and cytochrome P-450 reductase genes in the simulta-

neous transformation of corticosteroids and phenanthrene by *Cunninghamella elegans*. FEMS Microbiol. Lett. **261:**175–180.
19. **Kim YH, Lee C, Go H, Konishi K, Lee K, Lau PCK, Yu MH.** 2010. Decolorization of malachite green by cytochrome c in the mitochondria of the fungus *Cunninghamella elegans*. Arch. Biochem. Biophys. **494:**159–165.
20. **Singh R, Shivaprakash MR, Chakrabarti A.** 2011. Biofilm formation by zygomycetes: quantification, structure and matrix composition. Microbiology **157:**2611–2618.
21. **Gonzalez FJ.** 1988. The molecular biology of cytochrome P450s. Pharmacol. Rev. **40:**243–288.
22. **Wang RF, Cao WW, Khan AA, Cerniglia CE.** 2000. Cloning, sequencing, and expression in *Escherichia coli* of a cytochrome P450 gene from *Cunninghamella elegans*. FEMS Microbiol. Lett. **188:**55–61.
23. **Hammel KE.** 1995. Organopollutant degradation by ligninolytic fungi, p 331–346. *In* Young LY, Cerniglia CE (ed), Microbial transformation and degradation of toxic organic chemicals. Wiley-Liss, New York, NY.
24. **Shanmugam B, Luckman S, Summers M, Bernan V, Greenstein M.** 2003. New approaches to augment fungal biotransformation. J. Ind. Microbiol. Biotechnol. **30:**308–314.
25. **Gutiérrez-Correa M, Ludeña Y, Ramage G, Villena GK.** 2012. Recent advances on filamentous fungal biofilms for industrial uses. Appl. Biochem. Biotechnol. **167:**1235–1253.
26. **Bastiaens L, Springael D, Wattiau P, Harms H, DeWachter R, Verachtert H, Diels L.** 2000. Isolation of adherent polycyclic aromatic hydrocarbon (PAH)-degrading bacteria using PAH-sorbing carriers. Appl. Environ. Microbiol. **66:**1834–1843.
27. **Van Loosdrecht MCM, Lyklema J, Norde W, Zehnder AJB.** 1990. Influence of interfaces on microbial activity. Microbiol. Rev. **54:**75–87.
28. **White GF.** 1995. Multiple interactions in riverine biofilms—surfactant adsorption, bacterial attachment and biodegradation. Water Sci. Technol. **31:**61–70.
29. **Griffith PC, Fletcher M.** 1991. Hydrolysis of protein and model dipeptide substrates by attached and nonattached marine *Pseudomonas* sp. strain NCIMB 2021. Appl. Environ. Microbiol. **57:**2186–2191.
30. **Wicke D, Böckelmann U, Reemtsma T.** 2007. Experimental and modeling approach to study sorption of dissolved hydrophobic organic contaminants to microbial biofilms. Water Res. **41:**2202–2210.
31. **Wicke D, Böckelmann U, Reemtsma T.** 2008. Environmental influences on the partitioning and diffusion of hydrophobic organic contaminants in microbial biofilms. Environ. Sci. Technol. **42:**1990–1996.
32. **Harding MW, Marques LLR, Howard RJ, Olson ME.** 2009. Can filamentous fungi form biofilms? Trends Microbiol. **17:**475–480.
33. **Gutiérrez-Correa M, Villena GK.** 2003. Surface adhesion fermentation: a new fermentation category. Rev. Peru. Biol. **10:**113–124.
34. **Villena GK, Fujikawa T, Tsuyumu S, Gutiérrez-Correa M.** 2009. Differential gene expression of some lignocellulolytic enzymes in *Aspergillus niger* biofilms. Rev. Peru. Biol. **15:**97–102.
35. **Freeman WM, Walker SJ, Vrana KE.** 1999. Quantitative RT-PCR: pitfalls and potential. Biotechniques **26:**112–115.
36. **Rajagopalan S, Modak JM.** 1995. Evaluation of relative growth limitation due to depletion of glucose and oxygen during fungal growth on a spherical solid particle. Chem. Eng. Sci. **50:**803–811.
37. **Raghavarao KSMS, Ranganathan TV, Karanth NG.** 2003. Some engineering aspects of solid-state fermentation. Biochem. Eng. J. **13:**127–135.
38. **Hölker U, Lenz J.** 2005. Solid-state fermentation—are there any biotechnological advantages? Curr. Opin. Microbiol. **8:**301–306.